20

Optical imaging of combined fluorescent cellular spheroids and study of their growth under the influence of chemotherapy

© A.S. Sogomonyan[1,2], P.A. Kotelnikova[1], D.E. Demin[3], A.B. Mirkasymov[1,4], S.M. Deyev[1,4,5], A.V. Zvyagin[1,4,6]

[1] Shemyakin–Ovchinnikov Institute of Bioorganic Chemistry of the Russian Academy of Sciences,
117997 Moscow, Russia
[2] Institute of Engineering Physics for Biomedicine, National Research Nuclear University (MEPhI),
115409 Moscow, Russia
[3] Engelhardt Institute of Molecular Biology, Russian Academy of Sciences,
119991 Moscow, Russia
[4] Institute of Molecular Theranostics, Sechenov First Moscow State Medical University,
119991 Moscow, Russia
[5] Institute of Fundamental Medicine and Biology, Kazan Federal University,
420008 Kazan, Russia
[6] MQ Photonics Centre, Macquarie University,
2109 Sydney, Australia

e-mail: mirkasymov@phystech.edu

Received December 11, 2023
Revised January 19, 2024
Accepted March 05, 2024

The development of new drugs for cancer treatment requires a deeper understanding of carcinogenesis mechanisms and their more accurate reproduction. The creation of 3D cell models was an important step in the study of tumor stroma and the reconstruction of a relevant cancer model. Using 3D-printing and micromolding, we obtained polymer molds for the rapid formation of cellular spheroids, their long-term incubation and microscopy. The molds were used to create spheroids from cancer, stromal cells, and their combinations. In order to distinguish tumor and stromal cells during co-cultivation, they were transduced with genes of fluorescent proteins in different regions of the visible spectrum. Fluorescence microscopy allowed not only to observe the dynamics of spheroid growth, but also to evaluate separately the sensitivity of cancer and stromal cells to cytostatic therapy. The developed form simplifies the reconstruction of a relevant 3D cancer model and testing of cytotoxic drugs. The results obtained demonstrate the importance of optical methods in studying the antitumor efficiency of drugs.

Keywords: 3D-printing, multicellular tumor spheroids, fluorescent microscopy, cisplatin, chemotherapy.

DOI: 10.61011/EOS.2024.03.58745.29-24

Introduction

Efficient cancer control involves both the study of fundamental carcinogenesis mechanisms and the development and testing of drugs that inhibit tumor growth and development [1]. Immortalized human and mammalian cell lines (including cancer ones) have long been used in biology to study the vital processes of cells and characterize their properties, behavior, and, most importantly, the mechanisms underlying them. Cancer cells are studied in two-dimensional systems that have become classical *in vitro* models of behavior of adherent cell cultures [2].

Drugs undergoing preclinical trials must first be tested *in vitro* in cellular models. Having passed this initial experimental screening, candidates may then be tested *in vivo* [3]. This approach allows one to save time and resources by discarding ineffective drugs early on; and is also more ethical in relation to experimental animals. At the same time, the complexity of animal models often leads to ambiguous results and problems in their interpretation [4]. In comparison with the organismic level, three-dimensional cellular systems are much simpler in terms of design and organization of various biological processes, but, owing to the formation of a more complex architecture and the emerging diffusion restrictions, they also model the studied processes better than two-dimensional ones [5].

Cellular spheroids allow one to model the three-dimensional structure of a tumor along with intercellular junctions [6]. Instead of being attached to hard plastic, cells start to bind with each other and form an extracellular matrix, which may exert a significant influence on their behavior [7,8]. In addition, spheroids are characterized by a greater heterogeneity than two-dimensional models (the presence of gradients of nutrients, oxygen, and other molecules); as a result, a hypoxic region characteristic of many tumors is reproduced in the dense core of a spheroid [5,8,9]. Cellular spheroids are more resistant to chemotherapy than two-dimensional cultures [10]. Thus, test models of this kind make it possible to determine the ability of drugs to penetrate deep into a tumor and estimate more accurately the concentrations required for therapy.

However, three-dimensional systems of monocultures of cancer cells still cannot reproduce the structure of a tumor formed in combination with endothelial cells, fibroblasts, and immune cells [11]. It is known that co-culturing with stromal cells has a significant influence on invasion and proliferation [12,13], gene expression [14], and cell behavior [15].

Distinct labels need to be used in order to monitor different cell types in three-dimensional structures. Fluorescent labels are used widely in biological research as a simple tool for non-invasive monitoring [16]. Since different fluorescent labels feature absorption and emission in different ranges of the optical spectrum, they may be used for simultaneous visualization and differentiation of the objects under study [17]. Fluorescence microscopy is well-suited for monitoring of cellular spheroids expressing fluorescent proteins, since their fluorescence intensity allows one to assess cell viability and may be used for testing of anticancer drugs *in vitro* [18].

In the present study, we designed a 3D model of a photopolymer printing mold that is filled with agarose to create an optically transparent form in which cellular spheroids may be mass-cultured, tested, and monitored by fluorescence microscopy in a rapid and cost-effective manner. The developed molds were tested by producing spheroids from monocultures of EA.hy926 human endothelial cells, SKOVip-kat human ovarian cancer cells, EMT6/p mouse mammary cancer cells, L929 mouse fibroblasts, and their combinations. Fluorescence of the TurboFP635 (Katushka) red fluorescent protein expressed in tumor cells allowed us to assess the growth and viability of a spheroid over time. The effect of cisplatin on tumor and combined spheroids was studied. Fluorescence of cells at different wavelengths made it possible to monitor separately the effects of a model cytotoxic agent on cancer cells and fibroblasts inside a combined spheroid and revealed that fibroblasts in the outer part of the spheroid are the ones most affected by the chemotherapy drug, whereas tumor cells in the center of the spheroid are fairly resistant to it.

Materials and methods

Cell lines

SKOVip-kat (human ovarian carcinoma with stable expression of the TurboFP635 (Katushka) red fluorescent protein), EMT6/p (mouse mammary cancer), EA.hy926 (immortalized human umbilical vein endothelial cells), and L929 (mouse fibroblasts) cell lines were taken from the collection of the Laboratory of Molecular Immunology (Institute of Bioorganic Chemistry, Russian Academy of Sciences). Cells were cultured in DMEM (Dulbecco's modified Eagle medium) containing 10% FBS (fetal bovine serum) (HyClone, United States), 2 mM of L-glutamine (PanEco, Russia), and 50 units/ml/50 mkg/ml of penicillin-streptomycin (PanEco, Russia). Spheroids were cultured in colorless DMEM without phenol red (Gibco, UK) containing 10% bovine fetal serum (HyClone, United States), 2 mM of L-glutamine (PanEco, Russia), and 50 units/ml/50 mkg/ml of penicillin-streptomycin (PanEco, Russia). Cells and spheroids were incubated at 37°C and 5% CO_2.

Production of fluorescent cell lines

Fluorescent cell lines were obtained by transduction with lentiviral particles (LVT-TurboFP635 (Evrogen, Russia) for EMT6/p and LVT-TagGFP2 (Evrogen, Russia) for EA.hy926 and L929). To this end, 10^4 cells were seeded onto 6-well plates, and 100 μl of lentiviral particles with a titer of $0.5 \cdot 10^6$ T.E./ml were added. Cells with particles were incubated at 37°C and 5% CO_2, and the medium was replaced after 24 h. The efficiency of transduction was verified by flow cytometry and fluorescence microscopy. Transduced cells were reseeded onto culture flasks and cultured until they reached the exponential growth phase. Fluorescent cells were sorted using an S3e Cell Sorter (Bio-Rad Laboratories, United States). Following sorting, cells were expanded, cryopreserved, and stored at −150°C until experimentation.

Design of polymer molds

Autodesk Fusion 360 was used to model 81-well mold designed to be filled with agarose. Molds were printed using a FormLabs Form3 3D printer (United States) and the Formlabs Clear Resin photopolymer. Printed molds were cleaned of unpolymerized resin residues with ethanol in an ultrasonic bath, dried, and blown through. The molds were then irradiated by a 120 W UV diode lamp for 20 min to complete the polymerization process.

Production of spheroids

Polymer molds were filled with 900 μl of hot 1% agarose (PanEco, Russia) in colorless DMEM (Gibco, UK) without serum. Solidified agarose forms were transferred to 12-well plates (Corning, United States), and different numbers of cells (2000 or 3000 cells per well of an agarose form) in 190 μl of colorless DMEM were introduced into them. The plates remained at rest until the cells settled to the bottom of agarose forms. Following that, 1 ml of colorless DMEM with 10% FBS was introduced into the wells, and the plates were transferred carefully into an incubator with a humid environment, 37°C, and 5% CO_2 for the formation and growth of spheroids.

Cytotoxicity assessment

Resazurin test. The toxicity of cisplatin (antitumor drug) was assessed using the resazurin test. Spheroids were grown for 3 days in agarose forms at 37°C and 5% CO_2, and then the cytotoxic agent was added in various concentrations. On the 7th day, the medium was removed and 1 ml of a

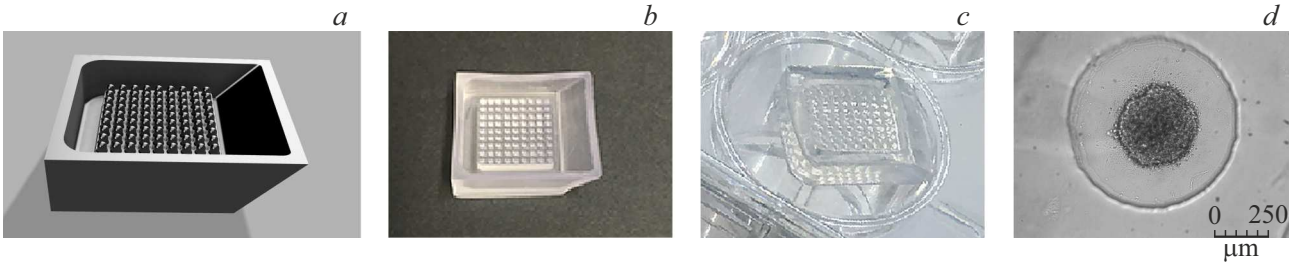

Figure 1. Formation of spheroids with the use of the designed mold: *a* — 3D model of the mold; *b* — mold printed by a 3D printer; *c* — solidified agarose form in a 12-well plate; and *d* — spheroid formed in a well of the agarose mold.

resazurin solution (13 mg/l) in the culture medium was added. This was followed by 24 h of incubation at 37°C and 5% CO_2. Next, the medium in the wells was then mixed by pipetting, and 100 μl of the medium were transferred to a 96-well plate (in triplicate). Fluorescence of a resazurin solution incubated under the same conditions in the wells of a plate with agarose forms without cells was used as the baseline. Measurements were carried out using an Infinite M100 Pro spectrophotometer (Tecan, Austria) at an excitation/emission wavelength of 570/595 nm. The concentration of cisplatin causing a 50% inhibition of cell growth (IC50) was determined with the use of GraphPad Prism 9.5.1.

Fluorescence of spheroids. The toxicity of the antitumor drug was assessed by detecting the fluorescence of Katushka TurboFP635 (hereinafter referred to as RFP) and GFP proteins. Spheroids were grown for 3 days in agarose forms at 37°C and 5% CO_2. Following that, cisplatin was added in various concentrations, and fluorescence of living cells in spheroids was assessed on the 7th day with the use of excitation and emission filters (545/30 and 610/75 nm for the red channel and 470/40 and 525/50 nm for the green channel). Fluorescence was detected with a Leica DMI6000B fluorescence microscope (Leica Microsystems, Germany). The fluorescence intensity of spheroids minus the background fluorescence was evaluated using ImageJ 1.51j8 in accordance with the following formula:

$$\text{CTCF} = \text{Integral density} - (\text{The area of the selected spheroid} \times \text{Average background fluorescence}).$$

Growth of spheroids. The dynamics of spheroid growth was assessed within the interval of 1-8 days after the introduction of cells into agarose forms. The needed transmission images of spheroids were obtained using a Leica DMI6000B microscope and the LAS AF 2.7.712402 software. The diameter of spheroids was measured in ImageJ 1.51j8.

Statistical analysis

All experiments were repeated at least six times. Results are presented as a mean ± standard deviation. The statistical significance between two groups was determined using the Welch's *t*-test for unequal variances. $P < 0.05$ and < 0.01 values were denoted with * and **, respectively.

Results and discussion

A 3D model (Fig. 1, *a* + stl file) of a container with a flat bottom and an inclined wall for photopolymer printing on a 3D printer (Fig. 1, *b*) was developed for quick and easy culturing of spheroids. When the mold was filled with molten agarose, a pedestal with a large number of protrusions within the container formed low-adhesive wells in solidified agarose for the formation of spheroids (Fig. 1, *c*). The size of the resulting agarose forms is optimized for the well of a 12-well culture plate and contains a square of 9 × 9 wells for spheroids. The flat bottom of the 3D model makes it easy to print directly on the 3D printer platform. The inclined wall allows one to pry and detach printed products from the printer platform and pry and pull out a solidified agarose form from this mold. The depth of wells is optimized so that spheroids remain securely within them when an agarose form is moved. The bottom of wells is made hemispherical so that settling cells form a single spherical conglomerate at the bottom of a well. The wells are 800 μm in diameter and allow for the formation of spheroids in a wide range of sizes (starting from $\sim$ 200 μm).

The pedestal in the mold forms wells in an agarose form that are filled with a cell-containing liquid. The pedestal surface is shaped in such a way (see Fig. S1) that cells settle precisely to the bottom of wells. Thus, with one movement of a pipette one may form a total of 81 spheroids containing approximately equal numbers of cells. The resulting agarose form is quite thin and transparent in the optical range, which makes it possible to monitor the formation of spheroids in a microscope directly in the agarose form in a 12-well plate (Fig.1, *d*).

The developed mold was used to form spheroids from various cell lines and their combinations. At the first stage, we studied the formation of multicellular spheroids from EA.hy926 human endothelial cells, SKOVip-kat human ovarian adenocarcinoma cells, and their mixture (Fig. 2). SKOVip-kat cells were chosen for the fact that our earlier studies [18] have demonstrated their efficiency in production of three-dimensional cellular models and drug screening.

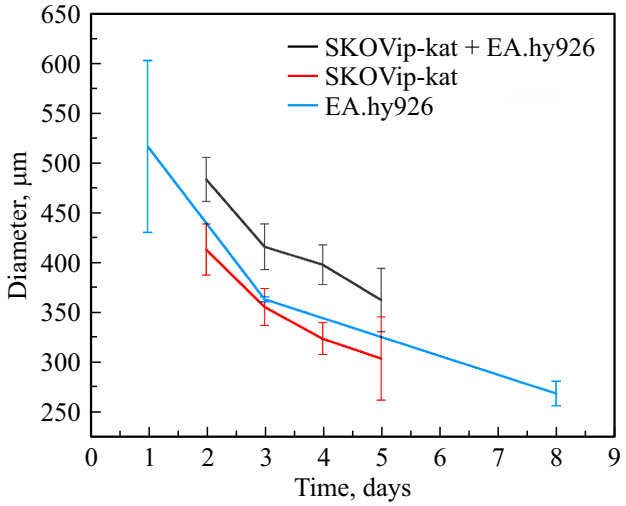

Figure 2. Size dynamics of forming spheroids. A total of 3000 cells per well.

Culturing SKOVip-kat and EA.hy926 cells in agarose forms, we observed a reduction in size and an increase in density of spheroids due to the formation of intercellular junctions and reorganization of the extracellular matrix [19]. As a result, spheroids of endothelial cells shrank from 516 ± 86 nm on the first day to 268 ± 12 nm on the eighth day, spheroids of ovarian cancer cells shrank from 413 ± 26 nm on the second day to 303 ± 42 nm on the fifth day, and spheroids formed from a mixture of cells contracted from 483 ± 22 nm on the second day to 362 ± 32 nm on the fifth day. The obtained spheroids of ovarian cancer cells had a fairly uniform spherical shape (see Fig. 2) and could be classified as dense spheroids [20]. Endothelial cells initially formed a looser structure than the one produced by ovarian cancer cells, but gradually contracted and compressed the spheroid. Similar behavior was noted in experiments on co-culturing of MDA-MB-231 metastatic breast cancer cells and MCF-10A non-tumorigenic epithelial cells [21].

Owing to the expression of RFP with an absorption/emission peak at a wavelength of 588/635 nm, spheroids of ovarian adenocarcinoma cells may be characterized not only by size (Fig. 2), but also by fluorescence intensity, which correlates with cell viability. We have demonstrated earlier that measurements of the spheroid fluorescence intensity may be an efficient method for assessing cell viability on a level with traditional colorimetric tests and flow cytometry [22]. It turned out that the fluorescence intensity of spheroids of SKOVip-kat cells and of their mixture with non-fluorescent endothelial cells changed slightly in the process of spheroid formation from day 2 to day 5 (see Fig. S3). Notably, the fluorescence of spheroids within one group varied much more significantly than their physical size, which translated into large standard deviations. It may be concluded that the number of cells varied insignificantly during the formation of a spheroid from SKOVip-kat cells, the formation of intercellular junctions, and its compaction. The lack of proliferation is also observed, e.g., in the case of formation of spheroids from MCF-7 breast cancer cells, hFIB fibroblasts, and their combination [23]. In addition, the difference in dynamics of changes in the physical size of a spheroid and the intensity of its fluorescence emphasizes that the physical size of a spheroid should not be regarded as an indicator of its viability.

A fluorescent model of mouse mammary cancer was developed to monitor tumor and stromal cells within a multicellular spheroid. We transduced EMT6/p mouse mammary cancer cells and L929 mouse fibroblast cells with red (RFP) and green (GFP) fluorescent proteins, respectively. Fluorescence at different wavelengths made it possible to distinguish cells in their mixture (see Fig. S4). It is evident that mammary cancer cells together with fibroblasts formed a fairly dense spheroid core, while only fibroblasts were found in the outer layer.

The resulting spheroids were used to test chemotherapy drugs. Cisplatin is a widely used drug for treatment of various types of cancer. Its primary mode of action involves binding to heterocyclic DNA bases and disrupting the replication process [24]. We studied the effect of different concentrations of cisplatin on spheroids of mouse mammary cancer cells by monitoring changes in the physical size of spheroids and their fluorescence intensity and assessing their viability using the resazurin test (Fig. 3).

In contrast to spheroids of SKOVip-kat and EA.hy926, spheroids of EMT6/p-RFP mouse mammary cancer cells initially formed a very dense conglomerate and did not shrink afterward; on the contrary, these spheroids increased in size, as is evident from a comparison of „day zero“and reference bars in the diagram in Fig. 3, *d*. At the same time, cisplatin in doses up to $10\,\mu$M did not affect the size of a spheroid, while the doses of 100 and $1000\,\mu$M had almost the same effect, inhibiting its growth and reducing the diameter from 371 ± 28 nm to almost 300 nm (compared to 264 ± 18 nm on day zero). Fluorescence microscopy yielded similar results at doses up to $10\,\mu$M. However, at higher concentrations, the fluorescence intensity dropped to 330 ± 33 arb.units (a.u.) and 433 ± 53 a.u., respectively, which is significantly lower than the fluorescence intensity of the reference spheroid (1642 ± 418 a.u.) and even the intensity on day zero (570 ± 88 a.u., Fig. 3, *c*). Thus, cisplatin had a significant effect at these doses, but fluorescence was not quenched completely, which may be attributed to the resistance of cells in the spheroid core or to residual protein fluorescence after cell death. In turn, the resazurin test, which is based on the reduction of resazurin into fluorescent resorufin due to intracellular enzymes and characterizes the metabolic activity of cells, revealed a significant effect even at small doses of the drug and complete suppression of metabolism at the maximum concentration (Fig. 3, *b*). For comparison, a cisplatin concentration of $\sim 3\,\mu$M induces an almost complete suppression of EMT6/p cell viability in a two-dimensional model [25].

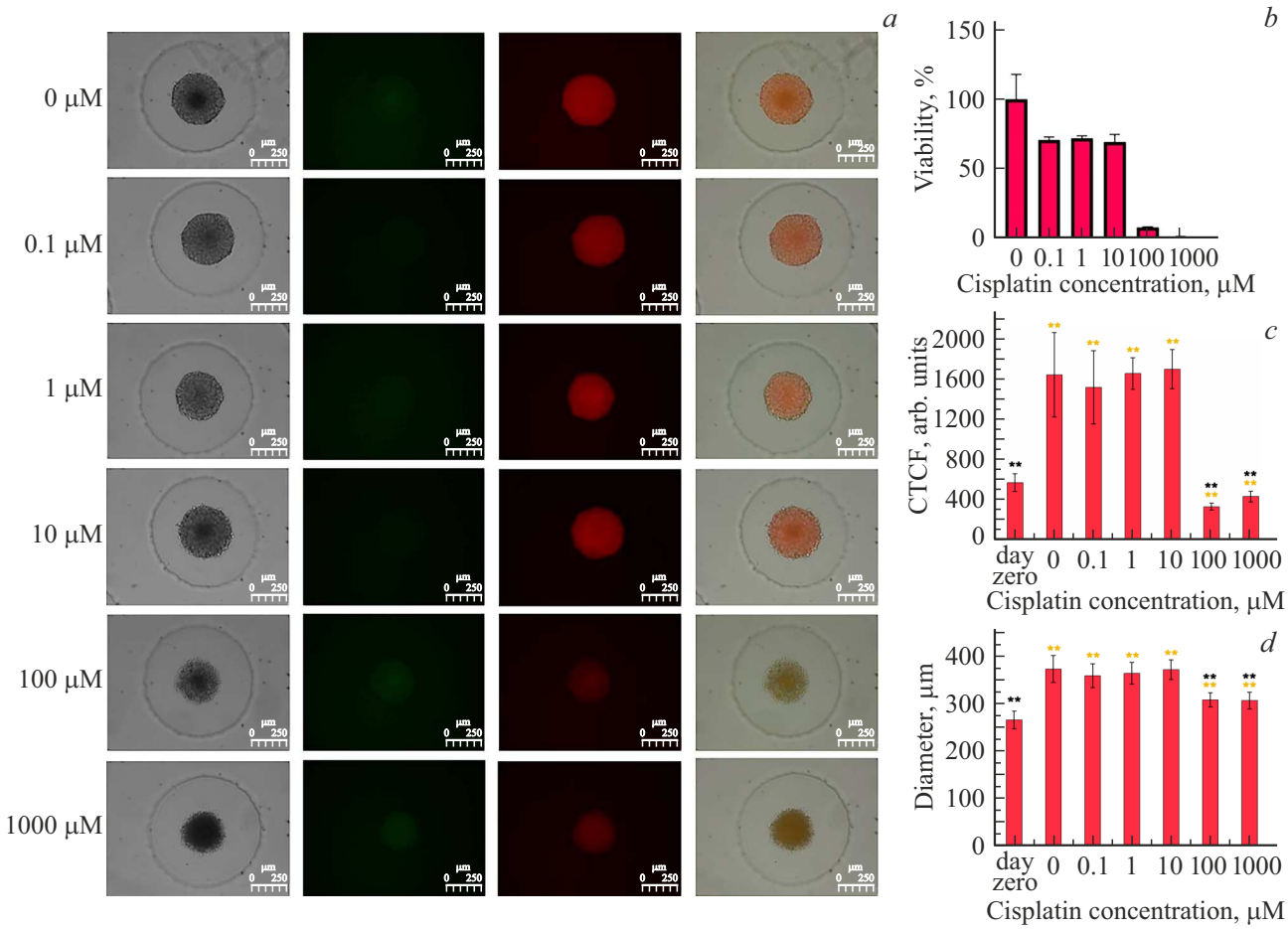

Figure 3. Effect of cisplatin on EMT6/p-RFP (mouse mammary cancer) spheroids. 2000 cells per well, day 7. *a* — Microscopic transmission images of spheroids, green and red fluorescence, overlay; *b* — resazurin test; *c* — fluorescence of spheroids in the red channel; and *d* — diameter of spheroids. The scale bar is 250 μm. ** — $P < 0.01$, Welch's *t*-test. Yellow * and black * denote the comparison with the „day zero" and zero-concentration bars, respectively.

The difference between the results of the resazurin test and fluorescence microscopy is probably attributable to the mode of action of cisplatin, which first inhibits metabolic activity and only then induces cell death [24]. In addition, the effect of cisplatin is due in part to the production of reactive oxygen species and, consequently, depends on the oxygen concentration [24], and the diffusion of oxygen, as well as that of resazurin and resorufin molecules, is constrained inside a spheroid. This confines the cytotoxic effect of cisplatin and the sensitivity of the resazurin test to the outer region of the spheroid, while fluorescent analysis is not subject to such restrictions.

No significant inhibition of spheroid growth was observed at cisplatin concentrations up to 10 μM in experiments with spheroids of L929-GFP mouse fibroblasts (Fig. 4). An increase in the drug dose led to a reduction in cell viability, a drop in fluorescence intensity to the zero-day level, and an almost complete cessation of physical growth (the resulting size was close to the zero-day level). However, a concentration increase to 1000 μM led to loosening of the spheroid and a significant growth of its diameter (compared to day zero), although metabolism was suppressed completely. This behavior, which differs from the one observed in experiments with spheroids of breast cancer cells, is probably attributable to the fact that the process of spheroid formation remains incomplete at the moment when the cytostatic is added: fibroblasts grow relatively slow, while proliferation in a spheroid of cancer cells already gives way to reorganization of the extracellular matrix. In addition, the lack of strict diffusion restrictions in fibroblast spheroids is evidenced by the fact that the cytotoxicity data turned out to be close to the results reported for a two-dimensional model [26].

At the next stage, we studied the effect of cisplatin on mixed spheroids of tumor and stromal cells (Fig. 5). The results of comparison of sizes of red and green regions of reference and zero-day spheroids suggested that the red core of a spheroid of breast cancer cells did not grow in size, although the fluorescence intensity increased, indicating cell proliferation. At the same time, green fibroblasts grew rapidly, reaching a diameter of 586 ± 26 μm (compared to 286 ± 14 μm on day zero) and raising

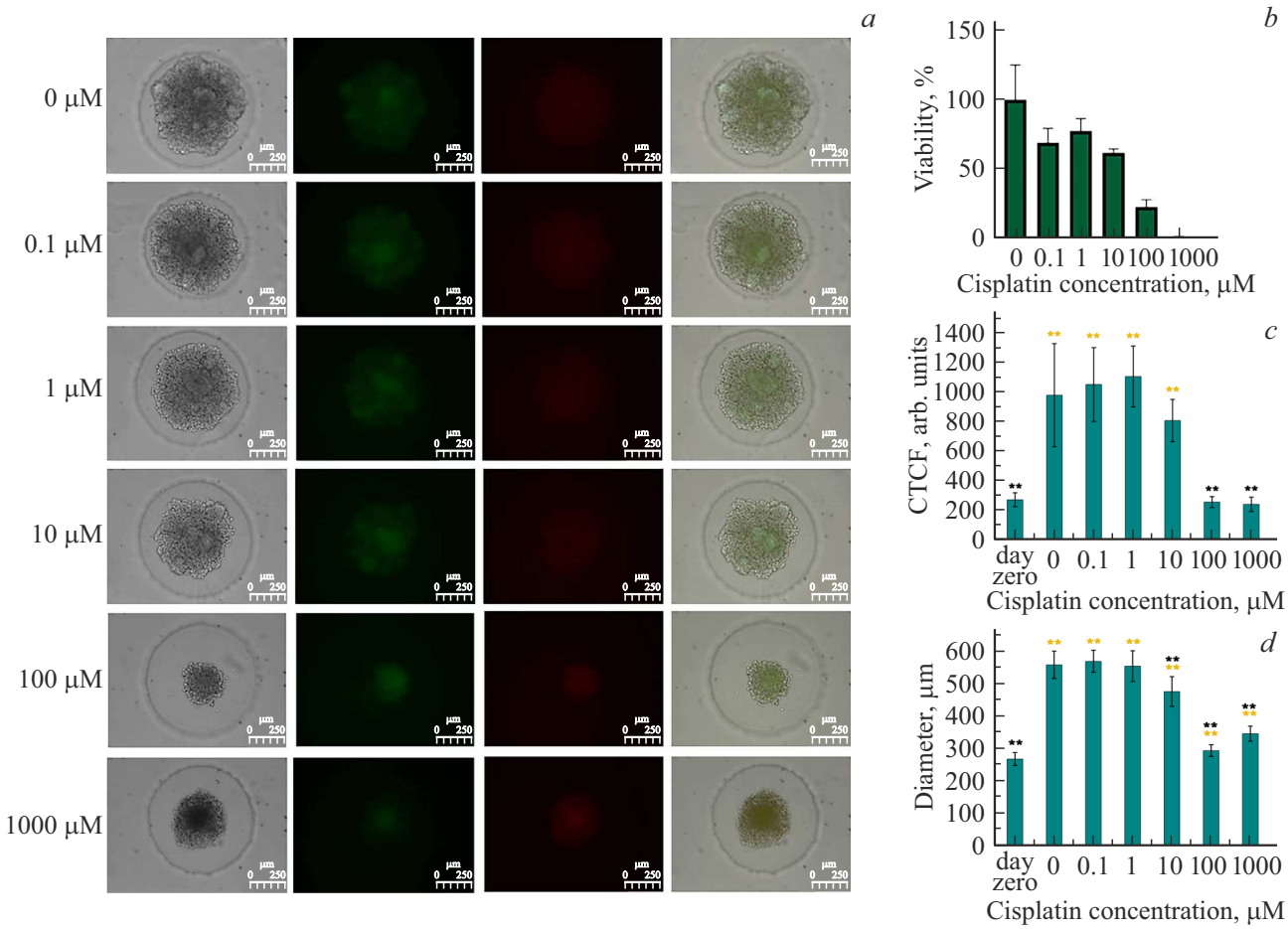

Figure 4. Effect of cisplatin on L929-GFP (mouse fibroblasts) spheroids. 2000 cells per well, day 7. *a* — Microscopic transmission images of spheroids, green and red fluorescence, overlay; *b* — resazurin test; *c* — fluorescence of spheroids in the green channel; and *d* — diameter of spheroids. The scale bar is 250 μm. ** — $P < 0.01$, Welch's *t*-test. Yellow * and black * denote the comparison with the „day zero" and zero-concentration bars, respectively.

the fluorescence intensity from 221 ± 48 to 1061 ± 58 a.u. Exposure to cisplatin in a concentration of 10 μM led to growth inhibition and a reduction in the size of the green region to 467 ± 28 μm; when the dose was increased, the size returned to zero-day levels. The diameter of the red region consisting of cancer cells changed only slightly depending on the concentration of the drug. The results of fluorescence analysis revealed a gradual reduction of green fluorescence intensity with an increase in cisplatin concentration (through to zero-day fluorescence values at the highest dose). Notably, the effect on breast cancer cells turned out to be significant only at a dose of 100 μM, which reduced the fluorescence intensity straight to 335 ± 63 a.u. (compared to 573 ± 91 a.u. in control and 460 ± 55 a.u. on day zero). However, a 10-fold dose increase did not lead to a reduction in fluorescence intensity. This probably provides evidence of the influence of residual fluorescence on analysis and the resistance of cells in the center of a spheroid. At the same time, the resazurin test, which characterizes the overall viability of the cell mixture, revealed a gradual reduction in viability with increasing dose (through to complete suppression of metabolism at the maximum concentration). Although the resazurin test is highly sensitive, it, just like other colorimetric tests, does not allow one to assess the effect of a drug on individual cells in a mixed spheroid or assess cell viability over time. Fluorescence revealed that fibroblasts were the cells primarily affected by cisplatin, while the drug in concentrations below 10 μM had no effect on breast cancer cells in the spheroid core.

A comparison of the effect of cisplatin on spheroids of different cell lines demonstrated that spheroids formed from a mixture of cells were more resistant to the chemotherapeutic agent than spheroids of monocultures (Fig. 6). The IC50 dose for spheroids of fibroblasts, breast cancer cells, and their mixture was 9 ± 5, 8 ± 4, and 17 ± 5 μM, respectively. Slight differences in sensitivity to antitumor therapy are likely related to the modulation of cell behavior in different three-dimensional models [27].

Thus, the assessment of viability of a spheroid by its physical size via transmission microscopy turned out to be inefficient and applicable only to spheroids of fibroblasts that

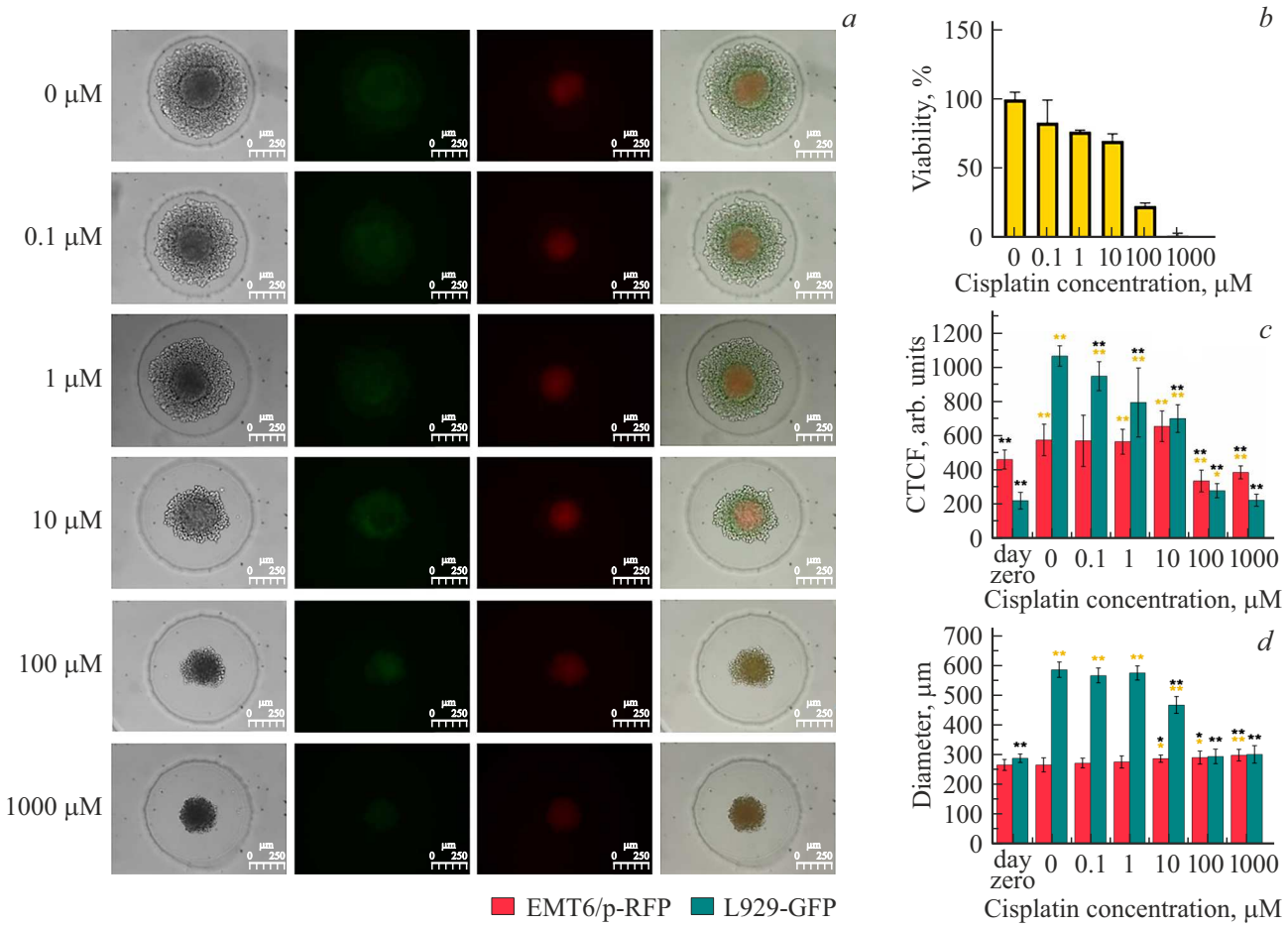

Figure 5. Effect of cisplatin on mixed EMT6/p-RFP+L929-GFP spheroids. 1000 + 1000 cells per well, day 7. *a* — Microscopic transmission images of spheroids, green and red fluorescence, overlay; *b* — resazurin test; *c* — fluorescence of spheroids in green and red channels; and *d* — diameters of green and red regions of a spheroid. The scale bar is 250μm. ** — $P < 0.01$, * — $P < 0.05$, Welch's *t*-test. Yellow * and black * denote the comparison with the „day zero" and zero-concentration bars of the corresponding channel, respectively.

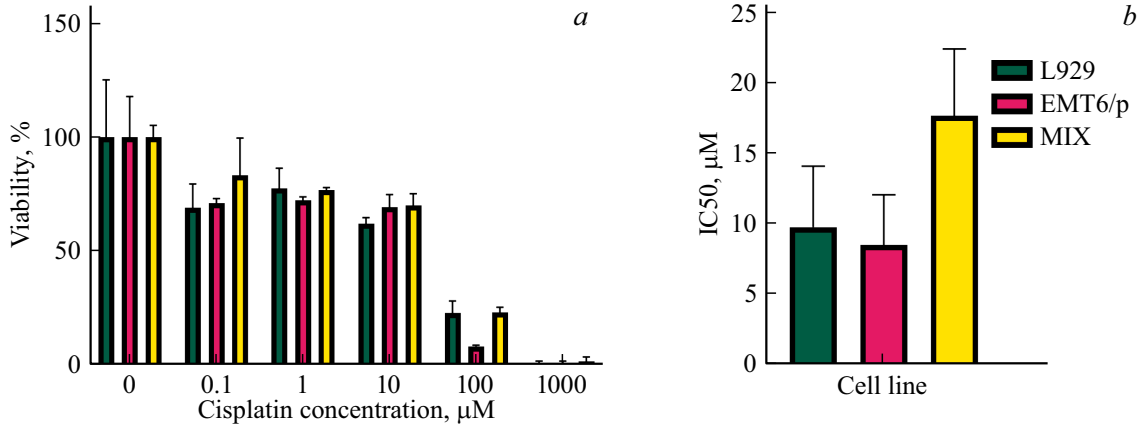

Figure 6. Comparison of the toxicity of cisplatin towards L929-GFP and EMT6/p-RFP spheroids and their combination determined using the resazurin test. Cell viability after exposure to cisplatin (*a*); IC50 of cisplatin for different spheroids (*b*).

grow rapidly under control conditions and, consequently, change in size significantly under the influence of cytostatics. Fluorescence microscopy allows one to assess the viability of cells expressing fluorescent proteins over time, although residual fluorescence makes it hard to perform accurate analysis when cells are almost completely dead.

The resazurin test has the capacity to distinguish the effects of even low concentrations of cytostatics, since changes in the metabolic activity of cells are manifested somewhat prior to their death. In addition, the lack of background activity of resazurin-reducing enzymes in dead cells allows one to use this method to study the effects of chemotherapy drugs in high concentrations. However, owing to hindered penetration of molecules deep into the aging and necrotic core of a spheroid and back, diffusion restrictions may affect the resazurin test results. Fluorescence microscopy is not subject to this limitation and also provides an opportunity to isolate the effects on different types of cells in a mixture and study them separately, provided that these cells are labeled with markers of different colors. Thus, each method has its own advantages and disadvantages; combining them, one may obtain a more complete picture of the phenomenon under study.

Conclusion

Using 3D printing technology, we developed a model that allows one to form and culture cellular spheroids en masse; monitor the morphology, behavior, and distribution of cells in a spheroid; and evaluate cell viability directly in the wells of a polymer mold.

The obtained model was tested by creating spheroids of different types of cells: ovarian and breast cancer cells, stromal cells (endothelium and fibroblasts), and their combinations. Having monitored their growth, we identified certain differences in the behavior of cells in the process of formation of spheroids. In addition, the sensitivity of spheroids formed from cancer and stromal cells and their mixture to cisplatin was tested, and IC50 was determined. Mixed spheroids and cancer cells in them were demonstrated to be highly resistant to cytostatics during co-culturing. Two methods for cell viability assessment (namely, fluorescence microscopy and the resazurin test) were compared. The obtained results provide a deeper insight into the methods for assessing the viability of spheroids and allow one to conduct studies on three-dimensional tumor models with minimum financial and labor costs.

Funding

The study was supported by the Russian Science Foundation, grant № 21-74-30016.

Conflict of interest

The authors declare that they have no conflict of interest.

References

[1] H. Zahreddine, K.L.B. Borden. Front. Pharmacol., **4**, 28 (2013). DOI: 10.3389/fphar.2013.00028

[2] P. Pellegrini, J.T. Serviss, T. Lundbäck, N. Bancaro, M. Mazurkiewicz, I. Kolosenko, Di Yu, M. Haraldsson, P. D'Arcy, S. Linder, A. de Milito. Cancer Cell Int., **18**, 147 (2018). DOI: 10.1186/s12935-018-0645-5

[3] V.O. Shipunova, M.M. Belova, P.A. Kotelnikova, O.N. Shilova, A.B. Mirkasymov, N.V. Danilova, E.N. Komedchikova, R. Popovtzer, S.M. Deyev, M.P. Nikitin. Pharmaceutics, **14**, 5 (2022). DOI: 10.3390/pharmaceutics14051013

[4] G. Blandino, F. Lo Sardo. J. Thorac. Dis., **11** (*Suppl 3*), S461–S464 (2019). DOI: 10.21037/jtd.2018.11.17

[5] G. Mehta, A.Y. Hsiao, M. Ingram, G.D. Luker, S. Takayama. J. Control. Release, **164** (2), 192–204 (2012). DOI: 10.1016/j.jconrel.2012.04.045

[6] S.J. Han, S. Kwon, K.S. Kim. Cancer Cell Int., **21** (1), 152 (2021). DOI: 10.1186/s12935-021-01853-8

[7] M. Kapałczyńska, T. Kolenda, W. Przybyła, M. Zajączkowska, A. Teresiak, V. Filas, M. Ibbs, R. Bliźniak, Ł. Łuczewski, K. Lamperska. Arch. Med. Sci., **14** (4), 910–919 (2018). DOI: 10.5114/aoms.2016.63743

[8] P.L. Olive, R.E. Durand. J. Natl. Cancer Inst., **84** (9), 707–711 (1992). DOI: 10.1093/jnci/84.9.707

[9] S.-H. Kim, H.-J. Kuh, C.R. Dass. Curr. Drug Discov. Technol., **8** (2), 102–106 (2011). DOI: 10.2174/157016311795563875

[10] Y.-S. Torisawa, A. Takagi, H. Shiku, T. Yasukawa, T. Matsue. Oncol. Rep., **13** (6), 1107–1112 (2005).

[11] R.M. Bremnes, T. Dønnem, S. Al-Saad, K. Al-Shibli, S. Andersen, R. Sirera, C. Camps, I. Marinez, L.-T. Busund. J. Thorac. Oncol., **6** (1), 209–217 (2011). DOI: 10.1097/JTO.0b013e3181f8a1bd

[12] M.P. Shekhar, J. Werdell, S.J. Santner, R.J. Pauley, L. Tait. Cancer Res., **61** (4), 1320–1326 (2001).

[13] M. Upreti, A. Jamshidi-Parsian, N.A. Koonce, J.S. Webber, S.K. Sharma, A.A. Asea, M.J. Mader, R.J. Griffin. Transl. Oncol., **4** (6), 365–376 (2011). DOI: 10.1593/tlo.11187

[14] N.N. Khodarev, J. Yu, E. Labay, T. Darga, C.K. Brown, H.J. Mauceri, R. Yassari, N. Gupta, R.R. Weichselbaum. J. Cell Sci., **116** (6), 1013–1022 (2003). DOI: 10.1242/jcs.00281

[15] M.J. Bissell, D. Radisky. Nat. Rev. Cancer, **1** (1), 46–54 (2001). DOI: 10.1038/35094059

[16] W.-T. Dou, H.-H. Han, A.C. Sedgwick, G.-B. Zhu, Y. Zang, X.-R. Yang, J. Yoon, T.D. James, J. Li, X.-P. He. Sci. Bull. (Beijing), **67** (8), 853–878 (2022). DOI: 10.1016/j.scib.2022.01.014

[17] S. Bhaumik, J. Boyer, C. Banerjee, S. Clark, N. Sebastiao, E. Vela, P. Towne. J. Cell. Biochem., **121** (12), 4974–4990 (2020). DOI: 10.1002/jcb.29827

[18] A.S. Sogomonyan, V.O. Shipunova, V.D. Soloviev, V.I. Larionov, P.A. Kotelnikova, S.M. Deyev. Acta Naturae, **14** (1), 92–100 (2022). DOI: 10.32607/actanaturae.11603

[19] I. Smyrek, B. Mathew, S.C. Fischer, S.M. Lissek, S. Becker, E.H.K. Stelzer. Biol. Open, **8** (1) (2019). DOI: 10.1242/bio.037051

[20] M. Vinci, S. Gowan, F. Boxall, L. Patterson, M. Zimmermann, W. Court, C. Lomas, M. Mendiola, D. Hardisson, S.A. Eccles. BMC Biol., **10**, 29 (2012). DOI: 10.1186/1741-7007-10-29

[21] Y.L. Huang, C. Shiau, C. Wu, J.E. Segall, M. Wu. Biophys. Rev. Lett., **15** (3), 131–141 (2020). DOI: 10.1142/s1793048020500034

[22] V.O. Shipunova, V.L. Kovalenko, P.A. Kotelnikova, A.S. Sogomonyan, O.N. Shilova, E.N. Komedchikova, A.V. Zvyagin,

M.P. Nikitin, S.M. Deyev. Pharmaceutics, **14** (1), (2021). DOI: 10.3390/pharmaceutics14010043
[23] E.C. Costa, V.M. Gaspar, P. Coutinho, I.J. Correia. Biotechnol. Bioeng., **111** (8), 1672–1685 (2014). DOI: 10.1002/bit.25210
[24] S. Dasari, P.B. Tchounwou. Eur. J. Pharmacol., **740**, 364–378 (2014). DOI: 10.1016/j.ejphar.2014.07.025
[25] M.R. Müller, K.A. Wright, P.R. Twentyman. Cancer Chemother. Pharmacol., **28** (4), 273–276 (1991). DOI: 10.1007/BF00685534
[26] E.E. Petrova, T.I. Valyakina, M.A. Simonova, R.L. Komaleva, S.V. Khaidukov, E.A. Makarov, D.Y. Blokhin, P.K. Ivanov, T.M. Andronova, V.A. Nesmeyanov. Int. Immunopharmacol., **6** (9), 1377–1386 (2006). DOI: 10.1016/j.intimp.2005.11.021
[27] O.I. Hoffmann, C. Ilmberger, S. Magosch, M. Joka, K.-W. Jauch, B. Mayer. J. Biotechnol., **205**, 14–23 (2015). DOI: 10.1016/j.jbiotec.2015.02.029

Translated by D.Safin